Magnetic Resonance Spectroscopy in Clinical Practice

Localization Techniques and Shimming

Markus von Kienlin
F. Hoffmann-La Roche Pharmaceuticals, Basel, Switzerland

1. Introduction

To measure *MR* spectra *in vivo*, one needs to control the spatial origin of the detected signals. For diagnostic purposes, one is not interested in a global spectrum representing the average metabolic composition of the whole patient, but in the metabolism of some specific organ or lesion. Because of the poor sensitivity, the issue of spatial localization is more delicate in *MRS* than in *MRI*, as the size of the selected volume typically has to be large, on the order of 1 cc or more. This often leads to signal contamination from adjacent tissue and to partial volume effects. A good control of the spatial origin therefore is crucial for a high quality of the acquired spectra.

2. Fundamentals

The one major physical frontier that in vivo MRS has to cope with is the limited spatial resolution as consequence of the inherently low sensitivity. Most other hurdles such as limited field-of-view or patient motion, to name just a few, are "merely" technological challenges. The latter may be very complex issues, which need a lot of clever engineering to overcome them. The limited resolution, however, is a fundamental physical limit, and current instrument designs are already close to the theoretical optimum. As long as there is no technological break-through, we will have to live with what is currently available: there is no hope to substantially increase sensitivity or spatial resolution. Fig. 1 gives a striking example of this limitation.

Often, one sees anatomical images with a box superposed, and it is claimed that a MR spectrum is originating from within that box. This is a very simplified representation. In reality, 'spatial localization' does not generate sharp borders. It rather produces a 'localization profile' that depends on the frequency profile of the selective pulses used in single voxel spectroscopy, or the so-called 'spatial response function' in spectroscopic imaging. The localization profile determines how much signal is lost within the voxel-of-interest (VOI), and by how much the localized spectrum is contaminated by signal originating from outside the VOI.

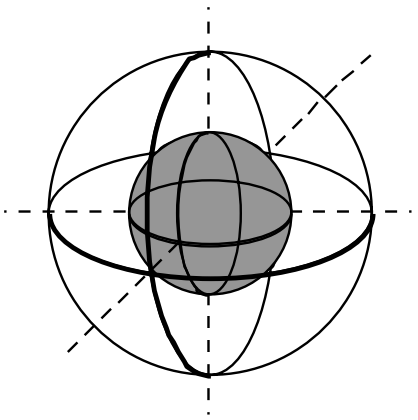

Fig. 1: *The duration necessary to measure the MR signal from a certain volume with a given signal-to-noise ratio (SNR) increases with the 6th (!) power of the linear dimension of the volume. For example, if a spectrum with a SNR of 10 can be acquired of the large sphere in 10 min, it takes* ***11 hours*** *to acquire a spectrum of the small sphere with half the diameter.*

3. Single voxel methods

The merit to have invented the first method to collect the MR spectrum from a well-delineated volume, based on the simultaneous use of selective RF pulses and pulsed gradients, goes to W. Aue and his "volume-selective excitation" (VSE) (*1*). VSE stimulated the development of a number of improved methods. These methods all make use of modulated, frequency-selective RF pulses played out in the presence of a pulsed gradient field.

To select a box, three selective pulses are applied one after the other, in the presence of mutually orthogonal field gradients. The intersection of the three excited planes is the (more or less) cube-shaped volume-of-interest (*VOI*, fig. 2). The so-called "single voxel methods" thus acquire the spectrum of a single selected volume within the sample – the detected signal originates from the intersection of the three slices. Single voxel methods have the following advantages: they are usually quite easy to implement, most modern MR instruments already have such measurement protocols implemented. Single voxel methods are quite reliable and reproducible, and they have a short minimal duration. Finally, they produce only a small amount of data, which facilitates data analysis.

The various single voxel methods have somewhat different properties, depending on whether the slice-selective pulses are 90°- or 180°-pulses. The three main representatives of these methods are ISIS (*2*), STEAM (*3-5*) and PRESS (*6*). Whenever applying slice selective pulses or readout gradients, this leads to a complication known as ***chemical shift artifact***. If various substances have different resonance frequencies due to their different chemical shift, the position of the selected slice will not be the same for all metabolites. Depending on the range of chemical shifts and the strength of the slice gradient, this displacement can be several millimeters or even centimeters: the broader the chemical shift range δ and the weaker the slice gradient G_s, the stronger the chemical shift artifact Δr:

$$\Delta r = \frac{B_0}{G_s} \cdot \delta \qquad \text{[Eq. 1]}$$

4. Spectroscopic imaging

In the same experimental duration that a single voxel method acquires the spectrum of a single *VOI*, spectroscopic imaging (*7, 8*) can collect the spectra data of a whole grid of many voxels. A spectroscopic image covers a whole plane (or a 3D volume) across the sample, with identical spatial resolution and the same signal-to-noise ratio. Just like *MRI*, this produces an image of the object. In contrast to *MRI*, each pixel of a metabolic image contains not a single gray value but a

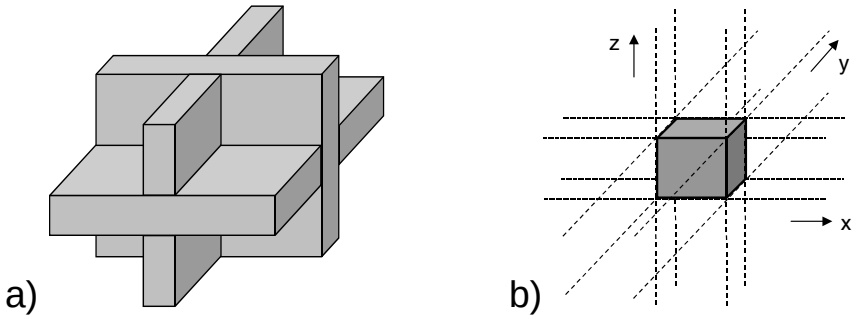

Fig. 2: *(a) Applying three selective pulses in the presence of three mutually orthogonal gradients, three intersecting slices are excited. (b) The volume-of-interest (VOI) is the intersection of the three slices.*

full *MR* spectrum. Such, the spatial distribution of specific metabolites can be visualized. If the *spatial distribution* of metabolites is of interest (rather than just the metabolic profile at one specific location), spectroscopic imaging is therefore a much more efficient way to record the data than single voxel methods.

These techniques are usually referred to as "*chemical shift imaging CSI"* or as "*spectroscopic imaging SI"*. Usually, they employ phase-encoding gradients to encode the spatial dimensions, and the *MR* signal is then collected in absence of any gradient in order to maintain the spectroscopic information (Fig. 3). Imaging-type methods, however, have the disadvantage that the shape of individual voxels is less well defined than in single voxel techniques. The shape of a voxel is indicated by the *'spatial response function'* (SRF), which indicates the weight with which every point in object space contributes to a local spectrum. The shape of the SRF is less 'square' than for single voxel methods, indicating signal loss within the VOI, and contamination from outside. The nominal spatial resolution is given by the 64%-amplitude of the SRF (*9*). In conventional spectroscopic imaging, the strong undulations of the baseline of the SRF cause very strong spatial contamination. Whenever possible, some scheme for acquisition weighting (rather than k-space filtering) should be used, in order to attenuate this contamination without giving up sensitivity (*10-14*).

The minimal duration of a conventional spectroscopic imaging study may be governed not by the time needed to achieve a sufficient signal-to-noise ratio, but by the time required to perform all the transients for all the different phase-encoding steps. This becomes a limitation in particular if a spectroscopic image with three spatial dimensions is to be collected. If for example a spectroscopic image with a spatial matrix of 32 x 32 x 16 were to be acquired, this would need a scan time of more than 4½ hours using a repetition time of TR = 1 sec – far too long to be tolerable by patients. Various schemes for ***fast spectroscopic imaging*** therefore have been devised to accelerate the data acquisition (provided that sufficient sensitivity is available). One of the easiest strategies already implemented on some clinical scanners is circular (or elliptical) *k*-space sampling: only data from the center of *k*-space are collected, its corners which contribute only little signal are omitted (*15*). Circular *k*-space sampling can be considered as the first stage of the afore-mentioned *k*-space weighting (*10-14*), and one should keep in mind that it does have an influence on the shape of the *SRF* and thus on the localization properties.

The most prominent methods of fast spectroscopic imaging employ pulsed magnetic field gradients during data acquisition to increase the speed of *k*-space coverage. This was proposed as

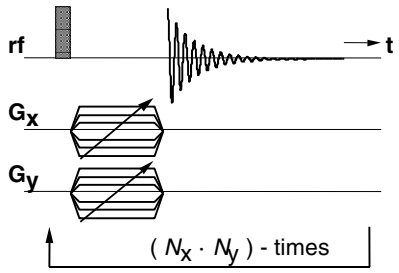

Fig. 3: *The basic pulse sequence for spectroscopic imaging in two spatial dimensions. After the RF excitation pulse, short gradient pulses are applied, which modulate the phase of the MR signal. The data are collected in the absence of any gradient, maintaining the spectral information. This procedure is repeated many times, ramping the gradient pulses independently in the two directions through all the values needed to obtain the desired spatial resolution. The metabolic image is reconstructed by Fourier transformation both in the spatial and the spectral dimensions.*

early as 1984 by the inventors of echo planar imaging, P. Mansfield *et al.* (*16-18*). Several modifications and improvements of this original technique have been proposed (*19-21*). In addition to these methods which are based on a (more or less) rectilinear sampling of *k*-space, spiral scanning schemes are very attractive, because of their even faster coverage of *k*-space and some inherent advantageous weighting of *k*-space (*22-24*). Many sequences for fast spectroscopic imaging have been reviewed by R. Pohmann *et al.* (*25*).

The main advantages and disadvantages of single voxel methods compared to spectroscopic imaging are summarized in the table below.

5. Field Homogeneity and Shim

The homogeneity of the main static magnetic field is another essential parameter which determines the quality and the success rate of spectroscopic studies *in vivo*. The homogeneity limits the line-width in the spectra and thus both the spectral resolution and the sensitivity. Furthermore, in ^{1}H-MRS, poor homogeneity renders water-suppression inefficient, which is one of the biggest hurdles for spectroscopic imaging.

The field homogeneity is not only determined by the magnet design, but it is perturbed by the inhomogeneous magnetic properties of the patient or sample, i.e. the magnetic susceptibility changes for instance at air-tissue interfaces. The higher the magnetic field, the stronger are the perturbations introduced by the patient. Some means to compensate these field deformations is therefore required, in particular on high-field instruments. In the early days of NMR, field homogeneity was optimized by introducing small iron plates to the magnet, the so-called 'shims'. Today, field homogeneity is rather adjusted by varying the current in additional coils which generate magnetic fields of appropriate geometry (*26*), but the name 'shimming' has remained.

It is essential that the total duration of a MRS examination remains acceptable. The former, time-consuming manual shim adjustment procedures therefore are more and more replaced by sophisticated, (semi-)automatic procedures (*27-34*). These have significantly improved both the comfort and the time needed to obtain optimal shim settings. It is important to realize, however, that shimming can only be a rather superficial, symptomatic cure: due to fundamental physical principles, it is not possible to fully compensate the local field perturbations by means of globally acting shim-coils.

	Single Voxel		Spectroscopic Imaging
++	localization in single scan (shim)	+	minimal duration long (N_x x N_y x TR)
-	chemical shift artifact	+/-	Spatial response function
+/-	only single voxel	++	full volume coverage
++	well implemented, robust	++	highly efficient
+	water-suppression relatively easy	--	water suppression shim-dependent
+	processing relatively easy	-	large amount of data

Table 1: *Comparison of some essential properties of single voxel localization vs. spectroscopic imaging*

6. References

1. W.P. Aue *et al.*, *J. Magn. Reson.* (1984), **56**: 350.
2. R.J. Ordidge *et al*., *J. Magn. Reson.* (1986), **66**: 283-294.
3. J. Frahm *et al*., *J. Magn. Reson.* (1987), **72**: 502-508
4. G.C. McKinnon, *Proceedings of the 5th ISMRM* (1986), 168
5. R. Kimmich *et al.*, *J. Magn. Reson.* (1987), **72**: 379-384
6. P.A. Bottomley, U.S.-Patent (1984), 4, 480, 228:0
7. T.R. Brown *et al.*, *Proc. Natl. Acad. Sci. USA* (1982) **79**: 3523-3526
8. A.A. Maudsley *et al.*, *J. Magn. Reson.* (1983) **51**: 147-152
9. M. von Kienlin *et al.* in "Spatially Resolved Magnetic Resonance" (P. Blümler et al. eds.), Wiley-VCH Weinheim (1998).
10. T.H. Mareci *et al.*, *J. Magn. Reson.* (1984) **57**: 157-163.
11. D.L. Parker *et al.*, *Med. Phys.* (1987) **14**: 640-645
12. R. Pohmann *et al.*, *Magn. Reson. Med.* (2001) **45**: 756-764
13. A. Greiser *et al., Magn. Reson. Med.* (2003) **50**: 1266-1275
14. B. Kühn *et al.*, *Magn. Reson. Med.* (1996) **35**: 457-464
15. A.A. Maudsley *et al., Magn. Reson. Med.* (1994) **31**: 645-651.
16. P. Mansfield, *Magn. Reson. Med.* (1984) **1**: 370-386.
17. D. Guilfoyle *et al.*, *Magn. Reson. Med.* (1985) **2**: 479-489.
18. D. Guilfoyle *et al.*, *Magn. Reson. Med.* (1989) **10**: 282-297.
19. D. Twieg, *Magn. Reson. Med.* (1989) **12**: 64-73.
20. P. Webb *et al.*, *Magn. Reson. Med.* (1989) **12**: 306-315.
21. S. Posse *et al.*, *Magn. Reson. Med.* (1995) **33**: 34-40.
22. E. Adalsteinsson *et al.*, *Magn. Reson. Med.* (1998) **39**: 889-898.
23. S. Sarkar *et al.*, *Magn. Reson. Imag.* (2002) **20**: 743-757.
24. B. Hiba *et al.*, *Magn. Reson. Med.* (2003) **50**: 1127-1133.
25. R. Pohmann *et al.*, *J. Magn. Reson.*(1997) **129**: 145-160.
26. F. Romeo *et al., Magn. Reson. Med.* (1984) **1**: 44-65.
27. P. Webb *et al., Magn. Reson. Med.* (1991) **20**: 113-122.
28. R. Gruetter, *Magn. Reson. Med.* (1993), **29**: 804-811.
29. H. Wen *et al., Magn. Reson. Med.* (1995) **34**: 898-904.
30. T. Reese *et al., J Magn. Reson. Imag*., (1995) **5**: 739-745
31. S. Kanayama *et al., Magn. Reson. Med.* (1996), **36**: 637-642.
32. J. Shen *et al., Magn. Reson. Med.* (1997), **38**: 834-839.
33. L. Klassen *et al., Magn. Reson. Med.* (2004), **51**: 881-887.
34. D. Spielman *et al., Magn. Reson. Med.* (1998), **40**: 376-382.